

# The Elimination Eyelash Iris Recognition Based on Local Median Frequency Gabor Filters

Jie Sun and Lijian Zhou

College of Communication and Electronic Engineering  
Qingdao Technological University  
Qingdao, 266033, P. R. China  
sj1979419@163.com,zhoulijian@qtech.edu.cn

Zhe-Ming Lu\*

School of Aeronautics and Astronautics  
Zhejiang University  
Hangzhou, 310027, P.R. China  
zheminglu@zju.edu.cn

Received September, 2014; revised January, 2015  
(Communicated by Zhe-Ming Lu)

---

**ABSTRACT.** *The orientation of iris texture will influence the iris recognition rate and the 2 dimensional Gabor filters (2-D Gabor) has better selectivity in orientation and frequency, so the multi-scales and multi directions 2-D Gabor filters can be used to extract the iris features. But there are many shortcomings such as long extraction feature time and high feature dimensions to use the traditional 2-D Gabor filters. So the elimination eyelash influence iris recognition based on median frequency Gabor filters is proposed in this paper. Firstly, the iris is preprocessed by iris and eyelash localization, normalization and elimination eyelash shelter. Secondly, 2-D Gabor filters with 3 scales and 8 directions are constructed to extract the feature of iris after preprocessing. Then using the Principal Component Analysis (PCA) and Linear Discriminant Analysis (LDA) further extract the feature and reduce the feature dimension. The experiment shows that the feature dimension is greatly reduced and the iris texture orientation is well considered by the proposed method compared with the traditional 2-D Gabor filters. The method in the paper can recognize the iris accurately and rapidly.*

**Keywords:** Iris recognition, 2 -D Gabor Filters, PCA, LDA.

---

**1. Introduction.** The iris recognition has been received more and more attention for its high accuracy, reliability and security over the last decade. Liu et al. [1] adopted discrete linear discriminate analysis to extract the iris feature and matched the feature by Hamming distance. Swati D. and Deepak [2] presented an efficient iris code classifier, built from phase features which used Gabor wavelets bandwidths. The final iris classifier consisted of a weighted contribution of weak classifier based on the Levenshtein distance between phase vectors of the respective iris images. Ahamed and Bhuiyan [3] provided a low complexity method for iris recognition in Curvelet transform domain. Yuan et al. [4] proposed to get iris texture orientation feature by 2D Gabor filters. This method only chose four directions of Gabor filters, so this method cannot well reflect the characteristics of the iris texture direction. Patil et al. [5] compared feature extraction algorithm based on PCA, Log Gabor Wavelet and Gabor Wavelet. Sun et al. [6] adopted the Curvelet transform to extract the iris feature. And then the iriss Curvelet features are mapped by

PCA and LDA to extract the further features. Ng et al. [7] proposed an iris recognition system using a basic and fast Haar wavelet decomposition method to extract the iris feature. In this method, they used Haar wavelet to decompose the iris region into four levels. And only the fourth level coefficients were converted into binary iris code. At last, the Hamming distance was used to recognize iris.

In this paper, the local Gabor filters are constructed through analysis of different frequency bands of 2D-Gabor filters effect on iris recognition rate and speed. Then PCA and LDA are used to further extract iris feature and reduce the feature dimension. First, the iris image is preprocessed by iris and eyelash localization, iris normalization and eyelash shelter elimination. Then choosing the filters of median frequency bands constructs the local median frequency Gabor filters to extract the iris local median frequency Gabor features. Next the PCA and LDA are used to further extract the feature and reduce the feature dimension. At last, the nearest neighbor classifier is adopted for iris recognition. Experimental results show that our method not only better extract orientation feature of the iris texture but also improve the recognition rate and feature extraction speed.

**2. Iris Image Preprocessing.** A captured iris image contains not only the interest region but also some unuseful part. In addition the iris's size and position will change during the different time, site, non-uniform illumination of image acquisition and the pupil zooming. In order to reduce these influences, the iris preprocessing of eyelash localization, image normalization and removal eyelash shading are needed before iris feature extraction.

**2.1. Iris and Eyelash Localization.** Iris segmentation is the first step of the iris preprocessing. We take an iris image with resolution of  $480 \times 640$  from CASIA-Iris-Syn of CASIA-Iris V4 for example and it is shown in Fig.1 (a). The iris texture is between the inner and outer two approximate circle boundary part, so the inner and outer boundaries should be extracted. The pupil's grayscale is the lowest and its boundary is circle. According to these characters, we use the threshold method to extract the iris inner boundary. Then the outer boundary is separated by Canny edge operator [8], the results of iris localization are shown in the Fig. 1(b). In addition, the eyelash shelter will influence the iris recognition result so the eyelash is also localized after iris localization. The result of eyelash localization is shown in Fig.1(c).

**2.2. Iris Image Normalization.** The non-uniform illumination and pupil zooming will cause the iris difference in size. So the normalization is used to remove the changes of iris size and position. Because the inner and outer boundaries are approach to the circle, we use the polar coordinates to unfold the iris part into rectangle [8]. And then the normalized iris image is zoomed into the same size. The normalized iris image can not only eliminate the influence caused by eye can't looking straight into the lens during the image acquisition, but also can eliminate the influence of pupil zooming caused by non-uniform illumination. The size of normalization image is  $100 \times 240$  and the result is shown in Fig.1 (d).

**2.3. Eyelash Shelter Elimination.** From the Fig.1 (c) we can see that the eyelash mainly influence the iris outer boundary and in the normalization image the eyelash area locates bottom as shown in Fig.1 (d). The eyelash will reduce the recognition rate and slow the feature extraction speed, so the eyelash should be eliminated [9]. In this paper, the highest point x-coordinate of the iris area of all the normalized images is used as threshold to eliminate the eyelash shelter. The result image is  $35 \times 240$  pixels and is shown in Fig.1 (e).

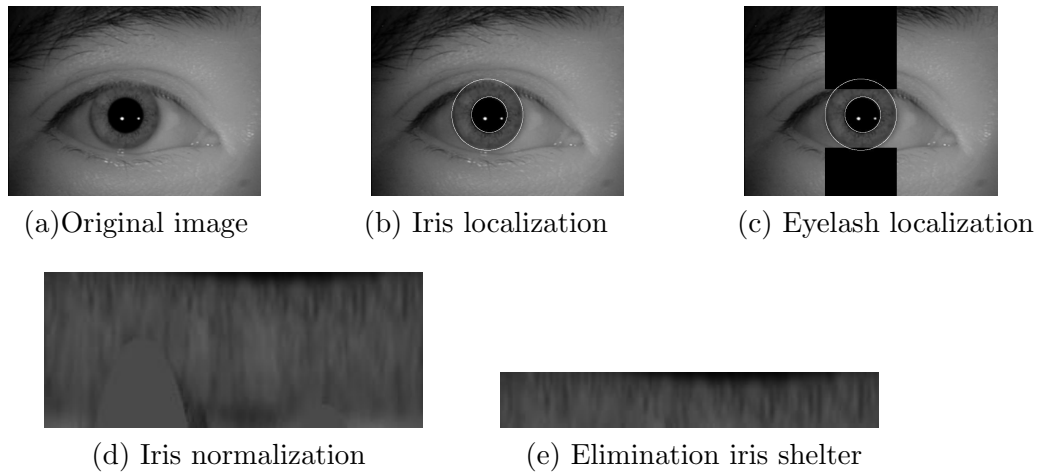


FIGURE 1. Results of Image Preprocessing.

Whether or not the eyelash shelter can influence iris recognition result and feature extraction time, we choose three kinds of normalized iris regions with different eye shelter percentage as samples to recognize iris. Region1 is the iris region without removal eyelash and it's size is  $100 \times 240$ . Region2 is the iris region with partial removal eyelash and it's size is  $50 \times 240$ . Region3 is the proposed iris region with removal all eyelash in this paper and it's size is  $35 \times 240$ . We choose 10 persons, 10 images per person from CASIA-Iris-Syn database of CASIA-Iris V4. Take randomly 1 to 9 images from every person as training set and take the rest as testing set. The results are shown in Table1. In addition, we also compare the feature extraction time of three regions. The results are shown in Table2.

TABLE 1. The recognition results of different iris region (%)

Number of samples of each person	Region1	Region2	Region3
1	37.78	37.34	36.56
2	49.52	49.45	49.67
3	68.14	68.20	68.23
4	75.89	75.90	75.93
5	90.43	90.61	90.74
6	95.00	95.67	95.98
7	96.14	96.21	96.32
8	96.67	97.00	97.34
9	98.34	98.59	98.72

TABLE 2. Feature extraction time of different regions

Region	Feature extraction time/ms
Region1	216.9
Region2	103.4
Region3	72.3

From the Table1 we can see that the iris region presented which remove the eyelash can get better recognition result. In addition, the feature extraction time of region1 needs 216.9ms and the region3 needs only 72.3ms which are shown in Table2.

**3. The Local Median Frequency Gabor filters Construction.** The iris image mainly contains some features such as wrinkles, crypts and stains which are made of different orientation and frequency information. The 2-D Gabor wavelet equips with better direction and frequency selectivity. So this paper uses the 2-D Gabor filters with multi-scale and multi-direction to extract the iris feature.

**3.1. Gabor Filter.** A group of different scales and directions filters compose the 2-D Gabor filters and the following formula is Gabor filter kernel function [10]:

$$\phi(k_{\mu,v}, z) = \frac{\|k_{\mu,v}\|^2}{\sigma^2} \tag{1}$$

$$\exp\left(-\frac{\|k_{\mu,v}\|^2 \|z\|^2}{2\sigma^2}\right) \left[ \exp(ik_{\mu,v}z) - \exp\left(-\frac{\sigma^2}{2}\right) \right] \tag{2}$$

whereis  $k_{\mu,v} = \begin{bmatrix} k_v \cos\varphi_\mu \\ k_v \sin\varphi_\mu \end{bmatrix}$ ,  $k_v = \frac{k_{max}}{f^v}$  denotes the Gabor filter direction,  $k_{max}$  is the biggest frequency (usually choose  $k_{max} = \frac{\pi}{2}$ ),  $v$  is scale label,  $f$  is interval factor  $f = \sqrt{2}$ ,  $z$  denotes the pixel position in spatial domain,  $\varphi_\mu = \frac{\pi\mu}{8}$  is Gabor filter scale factor,  $\mu$  is direction label. Generally, the traditional Gabor filters are composed of 5 scales  $v \in \{0, 1, 2, 3, 4\}$  and 8 directions  $\mu \in \{0, 1, 2, 3, 4, 5, 6, 7\}$ . The amplitudes of traditional Gabor filters are shown in Fig.2.

**3.2. The Local Median Frequency Gabor Filters Construction.** The convolution result of preprocessed image  $G$  and Gabor filter  $\phi$  is the Gabor feature of iris image, which is expressed as

$$M_{k_{\mu,v}}(z) = G(z) * \phi(k_{\mu,v}, z) \tag{3}$$

Where,  $M_{k_{\mu,v}}$  is the iris Gabor feature.  $M_{k_{\mu,v}}(z) = A_{k_{\mu,v}} e^{i\varphi_{k_{\mu,v}}}$ , where  $A_{k_{\mu,v}}$  and  $\varphi_{k_{\mu,v}}$  is amplitude and phase of  $M_{k_{\mu,v}}(z)$  separately. In this paper  $A_{k_{\mu,v}}$  is used as iris Gabor feature.

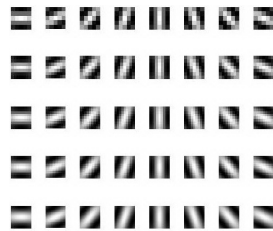


FIGURE 2. Amplitudes of traditional Gabor filters.

We take a preprocessed iris image Fig.1(e) as example that is filtered by Gabor filters with 5 scales and 8 orientations to get 40 Gabor feature images. The every Gabor feature image's size is  $35 \times 240$ . The amplitudes of Gabor feature images are shown in Fig.3, where the every row denotes the different scale and every column denotes the different orientation. If we make use of the 40 iris Gabor images to form the iris's feature vector

directly, the feature dimension is up to  $35 \times 240 \times 40 = 336000$  that is larger than  $35 \times 240 = 8400$  dimensions of the original image.



FIGURE 3. Iris Gabor feature images.

In order to reduce the Gabor feature dimension and feature extraction time, this paper selects only partial Gabor frequency bands information as the iris image's Gabor features according to the high frequency information mainly reflects the iris detail features and the low frequency information mainly reflects the rough features. From the Fig.3 we can see that the lowest frequency band (band 1) reflects mainly the approximate features of iris and contains the little specifics. The highest frequency band (band 5) reflects mainly the iris outline and contains much noise information. Neither of the lowest and highest frequency band information can well reflect the iris difference. On the contrary, we can see that the information of median frequency bands (bands 2 to 4) can not only reflect the iris coarse information but also the iris detail information. In order to verify our theoretical analysis, we choose the lowest frequency band, median frequency bands, highest frequency band and all frequency bands to construct the Gabor filters respectively and name the local low frequency Gabor filters (LFGF), local median frequency Gabor filters (MFGF), local high frequency Gabor filters (HFGF) and traditional Gabor filters (TGF) respectively. And then four kinds of Gabor filters are used to extract the iris Gabor features respectively. Here we randomly choose 50 persons, 10 images per person from CASIA-Iris-Syn database of CASIA-Iris V4. Our experiments adopt the iris image with resolution of size  $35 \times 240$  after preprocessing. We randomly take 1 to 9 images from every person as training set and take the rest as testing set. The recognition comparison results of every kinds Gabor filters are shown in Table3. From the Table3 we can see that the iris features extracted by MFGF gets higher recognition rate than the LFGF and HFGF. When the samples are small in size the recognition rate of MFGF is lower than TGF, but the recognition rate is higher with the samples increasing.

TABLE 3. The iris recognition results of 2D-Gabors with different frequency bands (%)

Number of samples of each person	LFGF	MFGF	HFGF	TGF
1	19.75	26.34	23.05	20.58
2	40.28	49.07	48.37	50.91
3	58.20	68.25	66.67	72.47
4	68.89	78.40	75.31	70.37
5	81.48	91.11	77.78	79.26
6	83.95	92.59	85.86	91.67
7	87.04	96.30	88.89	93.83
8	90.74	97.26	92.59	94.44
9	92.59	98.78	96.30	98.69

TABLE 4. Feature extraction time and feature dimension of different Gabor filters

Gabor filters filters	The number of filters	Feature dimension	Feature extraction time/ms
MFGF	24	201 600	72.3
TGF	40	336 000	116.5

In addition, MFGF feature extraction method greatly reduces the feature extraction time and feature dimensions compared the TGF and the experimental comparison results are shown in Table4.

**4. The Elimination Eyelash Iris Recognition Based on Local Median Frequency Gabor Filters.** The flow chart of elimination eyelash iris recognition based on local median frequency Gabor filters is shown in Fig.4. First, the acquisition iris images are preprocessed by iris and eyelash localization, normalization and elimination eyelash shelter. Second, constructing the local median frequency Gabor filters extracts the iris Gabor features of preprocessed iris images. Then using PCA and LDA further extract and reduce the dimension of iris Gabor features. At last, the nearest neighbor classifier is adopted for iris recognition.

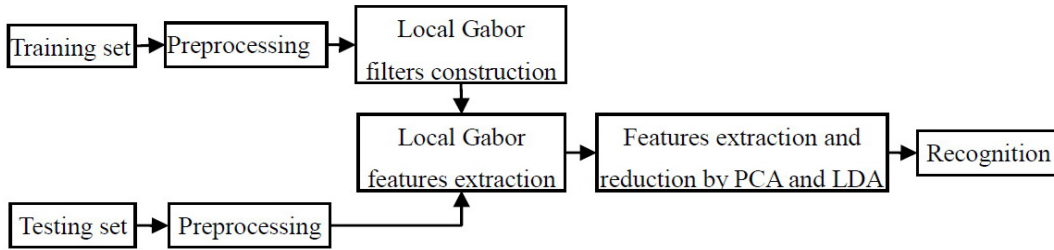


FIGURE 4. Algorithm flow chart.

Assume that there are samples in the training set  $X = [x_1, x_2, \dots, x_N]$ ,  $x_i$  is a column vector, representing the features of the  $i$ th iris. The specific algorithm steps can be illustrated as follows:

Step1. Preprocess each training image  $x_i$  by iris and iris eyelash localization, normalization and eyelash shelter elimination and get  $\tilde{x}_i$  with size of  $35 \times 240$  after preprocessing. Then, the iris feature set becomes  $\tilde{X} = [\tilde{x}_1, \tilde{x}_2, \dots, \tilde{x}_N]$ .

Step2. Construct local median frequency Gabor filters with 3 frequency bands and 8 directions namely  $v \in \{1, 2, 3\}$  and  $\mu \in \{0, 1, 2, 3, 4, 5, 6, 7\}$  in Eq.(1).

Step3. According to Eq.(2), each preprocessed image  $\tilde{x}_i$  is filtered by local median frequency Gabor filters constructed in step2 as follows

$$\hat{x}_i = \tilde{x}_i * \phi(k_{\mu,v}, z) \quad (4)$$

Thus, we can get the corresponding local median frequency Gabor features of each image to form the feature database  $\hat{X} = [\hat{x}_1, \hat{x}_2, \dots, \hat{x}_N]$ .

Step4. Transform feature database  $\hat{X}$  by PCA and LDA to form the feature sub space  $K$ . Get the low-dimensional training iris feature vector  $\hat{X}1$  by projecting the training set  $\hat{X}$  to the sub space  $K$ .

Step5. Accordingly, the input testing sample is also preprocessed and then extracted local median frequency Gabor features by local median frequency Gabor filters constructed

in step2. At last, project the local median frequency Gabor features of testing sample set to the feature sub space  $K$  formed in step4 to get the low-dimensional testing iris feature vector.

Step6. Adopt the nearest neighbor algorithm to recognize the iris.

**5. Simulation experiments and results.** In order to validate the performance of iris recognition based on local median frequency band Gabor filters proposed in this paper, we choose two iris image databases CASIA-Iris-Syn and CASIA-Iris-Lamp of CASIA 4.0 to perform the comparison experiments. We randomly select 50 persons, 10 images per person with gray scale of 256 from every iris database. For convenience, our experiments adopt the iris image with size of  $35 \times 240$  after preprocessing. In order to compare with other methods, we perform the proposed method (LMG+PCA+LDA), Curvelet+PCA+LDA [6] and Haar decomposition [7] (Haar) on the same database.

**5.1. Simulation Experiments Based on Syn Iris Database.** The irises textures of CASIA-Iris-Syn are synthesized automatically from a subset of CASIA-IrisV1. In this database, the intra-class variations introduced into the synthesized iris dataset include deformation, blurring and rotation. The example images of 2 persons, 5 images per person are shown in Fig. 5.

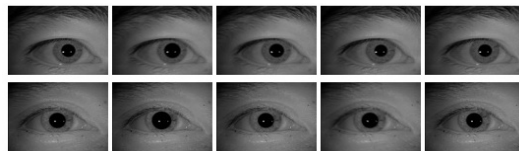


FIGURE 5. Original iris images of Syn.

We randomly choose 1 to 9 images from every person as training set and take the rest as testing set. To better evaluate the experimental results, we perform 10 runs for each experiment, and then calculate the average recognition rate (ARR) and variance (VR) of recognition rate. The comparison results are shown in Table 5. From the Table 5, we can

TABLE 5. Results on the Syn database(%)

Number of samples of each person	MFGF+PCA+LDA		Curvelet+PCA+LDA		Haar	
	ARR	VR	ARR	VR	ARR	VR
1	26.56	0.11	20.16	0.14	53.09	1.38
2	49.83	0.64	56.94	0.468	63.43	0.28
3	68.36	0.29	68.78	0.34	68.84	0.11
4	75.97	0.16	74.07	1.03	71.60	0.44
5	91.34	0.81	85.93	2.60	75.56	1.24
6	94.57	0.23	89.81	1.11	86.11	2.51
7	96.37	0.37	92.59	1.42	92.65	2.62
8	98.32	0.13	95.06	1.51	93.36	2.91
9	98.83	0.14	96.30	2.47	96.30	2.72

see that the recognition rate of the proposed method is higher than other methods. The highest rate of our scheme can reach 98.83% and it has a lower variance.

**5.2. Simulation Experiments Based on Lamp Iris Database.** CASIA-Iris-Lamp database contains right and left eye images of 411 classes and the size of each image is  $480 \times 640$ . In this paper, we choose the left eye images in this paper. The example images of 2 persons, 5 images per person are shown in Fig.6. We randomly choose 1 to 9 images as

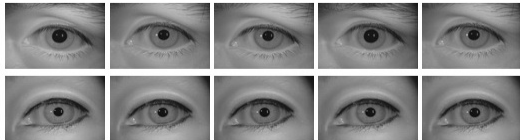


FIGURE 6. Original iris images of Lamp.

training set and take the rest as testing set. To better evaluate the experimental results, we perform 10 runs for each experiment, and then calculate the mean and variance of the results. The comparison results are shown in Table 6.

TABLE 6. Results on the Lamp database(%)

Number of samples of each person	MFGF+PCA+LDA		Curvelet+PCA+LDA		Haar	
	ARR	VR	ARR	VR	ARR	VR
1	13.58	0.05	15.64	0.11	45.68	0.14
2	46.30	0.16	52.78	0.19	61.57	0.38
3	73.54	0.10	72.49	0.10	71.96	0.76
4	85.80	0.12	83.95	0.32	83.33	0.67
5	91.56	0.06	89.15	1.12	85.19	1.09
6	93.52	0.22	91.67	1.45	84.26	1.98
7	95.06	0.27	92.59	0.89	87.28	1.02
8	96.30	0.39	95.32	0.76	90.70	0.37
9	98.96	0.06	96.78	0.34	92.98	0.54

From the Table 6, we can see that the recognition rate of the proposed method is higher than other methods. The highest rate of our scheme can reach 98.96% and it has a lower variance.

**6. Conclusions.** This paper proposes an iris recognition method based on local median Gabor filters. Firstly, the iris is preprocessed by iris and eyelash localization, normalization and eyelash shelter elimination. Secondly, the 2-D Gabor filters with 3 scales and 8 directions are constructed which make use of the median frequency characteristics of image and consider the orientation feature of iris texture. At last, the nearest neighbor method is used to recognized the iris. The experimental results show that the proposed method not only has higher recognition rate and better robustness, but also save the feature extraction time and reduce feature dimension.

**Acknowledgment.** This work was partially supported by the Zhejiang Provincial Natural Science Foundation of China under grant R1110006. The authors also gratefully acknowledge the helpful comments and suggestions of the reviewers, which have improved the presentation.



## REFERENCES

- [1] C. Liu, and M. Xie, Iris Recognition Based on DLDA, *18th International Conference on Pattern Recognition*, vol. 4, pp. 489-492, 2006.
- [2] S. Swati D. and G. Deepak, Iris Recognition Using Gabor, *Int. J. Computer Technology & Applications*, vol. 4, no. 1, pp. 1-7, 2013.
- [3] A. Ahamed and M. I. H. Bhuiyan, Low Complexity Iris Recognition Using Curvelet Transform, *International Conference on Informatics, Electronics & Vision (ICIEV)*, pp. 548-553, 2012.
- [4] W. Q. Yuan, Q. Feng, and L. Ke, Iris Recognition Method Based on Iris Texture Orientation Feature Extracted by 2D-Gabor Filter, *Application Research of Computers*, vol. 26, no. 8, pp. 3166-3168, 2009.
- [5] P. S. Patil, S.R.Kolhe, R.V.Patil and P.M.Patil, The Comparison of Iris Recognition using Principal Component Analysis, Log Gabor and Gabor Wavelets, *International Journal of Computer Applications*, vol. 43, no. 1, pp. 29-33, 2012.
- [6] J. Sun, Z. M. Lu and L. J. Zhou, Iris Recognition Using Curvelet Transform Based on Principal Component Analysis and Linear Discriminant Analysis, *Journal of Information Hiding and Multimedia Signal Processing*, vol. 5, no. 3, pp. 567-673, 2014.
- [7] T. W. Ng, T. L. Tay and S. W. Khor, Iris Recognition Using Rapid Haar Wavelet Decomposition, *2010 2nd International Conference on Signal Processing System*, vol. 1, pp. V1-820-823, 2010.
- [8] J. G. Daugman, High Confidence Visual Recognition of Persons by a Test of Statistical Independence, *IEEE Trans. on Pattern Analysis and Machine Intelligence*, vol. 159, no. 11, pp. 1148-1161, 1993.
- [9] M. Najafi and S. Ghofrani, A New Iris Identification Method Based on Ridgelet Transform, *International Journal of Computer Theory and Engineering*, vol.5, no. 4, pp. 633-637, 2013.
- [10] L. L. Shen, and L. Bai, Mutual Boost Learning for Selecting Gabor Features for Face Recognition, *Pattern Recognition Letters*, vol. 27, no. 15, pp. 1758-1767, 2006.